Wave Inversion Technology, Report No. 1, pages 61-69

Eigenwave based multiparameter traveltime expansions

Thilo Müller, Martin Tygel, Peter Hubral and Jörg Schleicher[1]

keywords: *imaging traveltimes*

ABSTRACT

Three different 2-D traveltime approximations for rays in the vicinity of a fixed zero-offset ray are presented and analyzed. All traveltimes are given as three-parameter expansions involving the emergence angle of the zero-offset ray with respect to the surface normal, as well as two wavefront curvatures associated with the zero-offset ray, namely the normal wave and normal-incidence-point wave. A comparison of all three multiparameter traveltime expansions is carried out.

INTRODUCTION

Traveltimes of rays in the (paraxial) vicinity of a fixed (central) ray can be described by certain parameters which refer to the central ray only. The traveltime approximations directly obtained from paraxial ray theory are the parabolic and the hyperbolic expansions ((Schleicher et al., 1993)). An appealing alternative traveltime description, has been recently proposed by (Gelchinsky et al., 1997). In this new representation, the paraxial rays can be specified so as to focus at a certain point of the zero-offset ray or at an extension to this ray. For this reason, Gelchinsky's expression has been referred to as the multi-focus traveltime. In the second-order approximation the multi-focus traveltime agrees with its parabolic and hyperbolic counterparts. In this paper we provide simple derivations of all above mentioned formulas and examine their behaviour for a synthetic model.

THE TRAVELTIME EXPANSION FORMULAS

In the following, we refer to Figure 1.

[1]**email:** Thilo.Mueller@physik.uni-karlsruhe.de

Figure 1: Construction of the focusing wave. Shown is the normal ray from X_0 to NIP. Also depicted are two of all possible paraxial rays (SRG and $\overline{SRG}$) that intersect this central ray at a common focus point P. These set of rays defines a fictitious wave called the focusing wave that starts at X_0 with the wavefront Σ_S, focuses at P, is reflected at the reflector Σ and emerges again at X_0, now with the wavefront Σ_G.

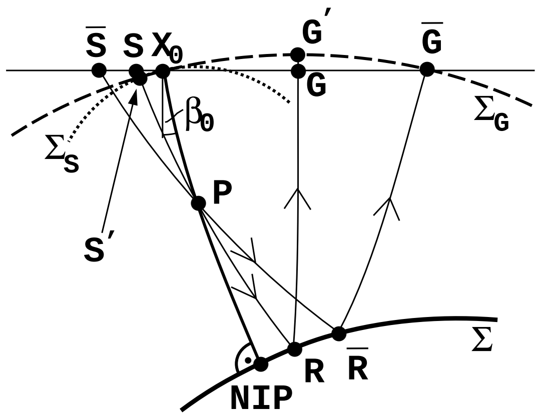

Parabolic and hyperbolic traveltimes

Following the formalism of (Bortfeld, 1989) tailored to the present two-dimensional propagation, the 2×2 *propagator matrix*

$$T = \begin{pmatrix} A & B \\ C & D \end{pmatrix} \tag{1}$$

describes a first-order relationship

$$\begin{cases} \Delta x_G = A\ \Delta x_S + B\ \Delta p_S\ , \\ \Delta p_G = C\ \Delta x_S + D\ \Delta p_S\ , \end{cases} \tag{2}$$

where Δx_S and Δx_G are the source and receiver offsets of the paraxial ray with respect to the central ray. Δp_S and Δp_G denote the corresponding slowness projection differences of these rays onto the seismic line at the initial and end points, respectively. All these quantities are measured with respect to a fixed coordinate system attached to the tangent to the measurement surface at X_0. Using the fact that the down-going segment of the normal ray connecting X_0 to NIP is the reverse ray to the up-going segment from NIP to X_0 and along similar lines as in (Bortfeld, 1989), we can find the useful relations

$$A = D = (K_{NIP} + K_N)/(K_{NIP} - K_N)\ , \tag{3}$$

$$B = (\cos^2 \beta_0 / v_0)\ [2/(K_{NIP} - K_N)]\ , \tag{4}$$

where v_0 is the velocity at X_0, K_{NIP} and K_N are the curvatures of the Eigenwaves NIP-wave and N-wave ((Hubral, 1983)), respectively. The so-called *symplecticity* property of propagator matrices, namely the relation $AD - BC = 1$, produces the remaining element C. Following (Bortfeld, 1989) or (Schleicher et al., 1993), we use midpoint and offset coordinates

$$x_m = \frac{\Delta x_G + \Delta x_S}{2}, \quad h = \frac{\Delta x_G - \Delta x_S}{2}, \tag{5}$$

to find for the parabolic traveltime

$$t_{par}(x_m, h) = t_0 + (2\sin\beta_0/v_0)\ x_m + (\cos^2\beta_0/v_0)\ (K_N\ x_m^2 + K_{NIP}\ h^2)\ , \qquad (6)$$

and for the hyperbolic traveltime

$$t_{hyp}^2(x_m, h) = [t_0 + (2\sin\beta_0/v_0)\ x_m]^2 + (2t_0\cos^2\beta_0/v_0)\ (K_N\ x_m^2 + K_{NIP}\ h^2)\ . \qquad (7)$$

In the above formulas, t_0 denotes the two way traveltime along the central ray.

MULTI-FOCUS TRAVELTIME

For the computation of the multi-focus traveltime we consider the bundle of primary reflection rays that focus a fixed point P. As depicted in Figure 1, we imagine that all these rays describe a certain fictitious wave, which we call a *focusing wave*. For each of the focusing rays $SPRG$, the source and receiver offsets Δx_S and Δx_G are no longer independent but are related by the condition that it has to pass through the fixed point P. Our problem is to find a traveltime approximation for the rays paraxial to the central ray and satisfying this *focusing condition*. Let us now designate by Σ_S and Σ_G the initial and final wavefronts of the focusing wave, respectively. We approximate Σ_S by a circle, calling its curvature K_S. Similarly, we define the curvature K_G of the circular approximation of the wavefront Σ_G at X_0. Let S' and G' denote the points where the focusing ray $SPRG$ hits the initial and end wavefronts Σ_S and Σ_G, respectively. Let us now consider the paraxial ray $SPRG$ to be constituted by two ray segments. The first one connecting S to P and the second one describes the remaining path of the reflected ray from P to R and from there to G. We may then write the traveltimes t_S and t_G along these two ray segments SP and PRG in the form

$$t_S = t_{0S} + \Delta t_S\ , \quad t_G = t_{0G} + \Delta t_G\ , \qquad (8)$$

where t_{0S} and Δt_S are the traveltimes along the ray segments $S'P$ and SS', respectively. The definitions of t_{0G} and Δt_G are analogous. Note that t_{0S} coincides with the traveltime along the central-ray segment from X_0 to P and t_{0G} coincides with the sum of the traveltimes along the central-ray segment from P to NIP and from NIP to X_0. Approximating the ray segments SS' and $G'G$ by straight lines, we find, using simple geometrical arguments

$$\Delta t_S = \frac{1}{K_S v_0}\left[\sqrt{1 + 2K_S\sin\beta_0\Delta x_S + \Delta x_S^2 K_S^2} - 1\right] \qquad (9)$$

$$\Delta t_G = \frac{1}{K_G v_0}\left[\sqrt{1 + 2K_G\sin\beta_0\Delta x_G + \Delta x_G^2 K_G^2} - 1\right]. \qquad (10)$$

Our problem reduces, thus, to the determination of the curvatures K_S or K_G. For that matter, we find it convenient to draw the line normal to the central ray at point P and consider it as an *auxiliary interface*. We also set a local coordinate system at P to locate ray points and slowness projections which refer to rays arriving to and leaving from this auxiliary interface. We may now define the two auxiliary propagator matrices

$$T_1 = \begin{pmatrix} A_1 & B_1 \\ C_1 & D_1 \end{pmatrix} \; , \quad T_2 = \begin{pmatrix} A_2 & B_2 \\ C_2 & D_2 \end{pmatrix} \; , \tag{11}$$

which correspond to the two (central) ray segments from X_0 to P and from P to X_0 being reflected at NIP, respectively. For the two segments SP and PRG of the paraxial ray $SPRG$ (see Figure 1), the two matrices T_1 and T_2 set up the first-order relationships

$$0 = A_1\,\Delta x_S + B_1\,\Delta p_S \; , \tag{12}$$

$$\Delta p = C_1\,\Delta x_S + D_1\,\Delta p_S \tag{13}$$

and

$$\Delta x_G = 0 + B_2\,\Delta p \; , \tag{14}$$

$$\Delta p_G = 0 + D_2\,\Delta p \; . \tag{15}$$

Note that the focusing condition at point P has been incorporated in the above equation systems by imposing the ray offsets of both segments SP and SRG at P to vanish and their slowness projections at P to be equal (denoted by Δp). Using simple algebra on the above equations provides a relationship between the source and receiver offsets for a focusing ray, namely

$$\Delta x_G = -\,(B_2/B_1)\,\Delta x_S \; . \tag{16}$$

The traveltimes t_1 and t_2, along the rays SP and PRG, can be written following (Bortfeld, 1989) and (Hubral, 1983) as

$$\begin{aligned} t_1 &= t_{0S} + \frac{\sin\beta_0}{v}\Delta x_S + \frac{\cos^2\beta_0 K_S}{2v}(\Delta x_S)^2 \; , \\ t_2 &= t_{0G} + \frac{\sin\beta_0}{v}\Delta x_G + \frac{\cos^2\beta_0 K_G}{2v}(\Delta x_G)^2 \; , \end{aligned} \tag{17}$$

where t_{0S} and t_{0G} are the traveltimes along the respective central rays and

$$K_S = \frac{A_1}{B_1}\frac{v}{\cos^2\beta_0} \; , \quad K_G = \frac{D_2}{B_2}\frac{v}{\cos^2\beta_0} \; , \tag{18}$$

are the wavefront curvatures of the fictitious focusing wave at the initial point S and end point G, respectively. To determine the quantities A_1/B_1 and D_2/B_2, we make use of the *chain rule* of propagator matrices $T = T_2\,T_1$, as well as the symplecticity relations $A_i\,D_i - B_i\,C_i = 1$, $(i = 1, 2)$. After some algebraic manipulation of the above equations, we find the relations $K_S = (A + B_2/B_1)/B$ and $K_G = (A + B_1/B_2)/B$. Together with the focusing condition, as well as the representations (3) and (4) of A and B in terms of K_N and K_{NIP}, we obtain the final result

$$K_S = \frac{1}{1-\gamma}\,(K_N - \gamma\,K_{NIP}) \quad \text{and} \quad K_G = \frac{1}{1+\gamma}\,(K_N + \gamma\,K_{NIP}) \; , \tag{19}$$

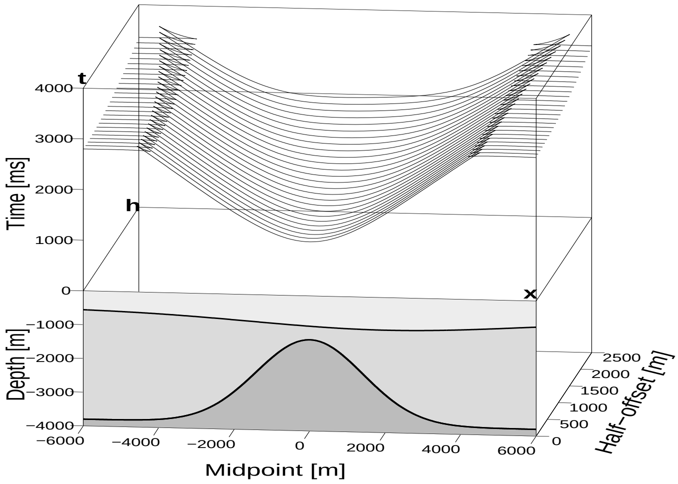

Figure 2: The upper part shows the traveltime surface in the midpoint-half-offset domain as computed for the velocity structure depicted in the lower part.

where

$$\gamma = (\Delta x_G - \Delta x_S)/(\Delta x_G + \Delta x_S) \tag{20}$$

is the *focusing parameter* of (Gelchinsky et al., 1997). Now, putting all intermediate results together, we come up with the multi-focus formula

$$t_{multi} = t_S + t_G \ , \tag{21}$$

inserting the relationships (8), (9), (10), (19) and (20).

NUMERICAL EXPERIMENTS

In order to illustrate the presented traveltime approximations, we have chosen a synthetic 2D-model, where a dome-like structure is overlain by a smoothly curved interface as shown in Figure 2. Layer velocities are assumed to be constant, where v_1=2300m/s and v_2=2800m/s correspond to the first and second layer, respectively. The reflection response of the dome structure has been calculated by a ray tracing algorithm. The corresponding traveltime surface in dependence of midpoint and half-offset coordinates, x and h, respectively, is displayed in Figure 2 as well.

For a fixed midpoint coordinate x=–455m the traveltime approximations (given in equations (6), (7) and (21)) are calculated for the reflected wave field from the dome-like reflector. Therefore the angle of incidence β_0 of the zero offset ray, as well as the curvatures K_{NIP} and K_N of the two eigenwaves need to be known. For the case of a known velocity model, simple geometrical considerations yield these parameters. In the present case these parameter are: $\beta_0 = 33.3^o$, $K_{NIP} = 2.06 \cdot 10^{-4} 1/m$ and $K_N =$

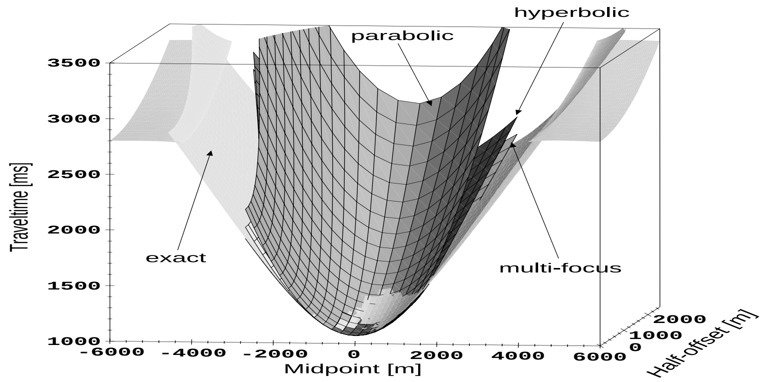

Figure 3: The exact traveltime curve of Figure 2 is compared to the three traveltime approximations discussed in the text, as computed for an arbitrarily chosen midpoint.

$5.43 \cdot 10^{-5} 1/m$. The resulting traveltime surfaces are given in Figure 3. In order to make comparison with the exact traveltimes visual, 2D-slices of the traveltime surfaces for constant half-offsets h=0m, 500m, 1000m, 2000m are depicted (see Figure 4).

For the zero-offset (h=0m) case it can be seen that all three traveltime approximations fit very good to the exact curve. Even away from the chosen midpoint (x=–455m) the results are good. For intermediate half-offset (h=500m, 1000m) the approximations are still very good for the hyperbolic and the multi-focus representation. The parabolic approximation is good at the chosen midpoint but deviates from the exact curve for distant midpoint coordinates. For larger offset (h=2000m) all three traveltime representations deviate from the exact traveltime response. However, the multi-focus traveltime approximation gives still a good fit on the branch for positive midpoints.

CONCLUSION

Second- and higher-order traveltime expansions have been of great use for seismic processing for a long time. For CMP data, the one-parameter, hyperbolic NMO-traveltime is still routinely used for velocity analysis, stacking and inversion.

Alternatively, using a full multi-coverage data set along a seismic line, three-parameter, second-order traveltime expansions can be used. In this paper, we have compared the parabolic and hyperbolic traveltimes derived from paraxial ray theory (see, e.g., (Bortfeld, 1989); (Schleicher et al., 1993)) with the multi-focus traveltime of (Gelchinsky et al., 1997). For this purpose, we have reformulated the three approximations in terms of the same three parameters, namely the emergence angle of the normal ray, as well as the wavefront curvatures of the N- and NIP- eigenwaves introduced by (Hubral, 1983).

For various tested examples, the hyperbolic and multi-focus approximations gave, as expected for seismic models consistently better results than the parabolic traveltime.

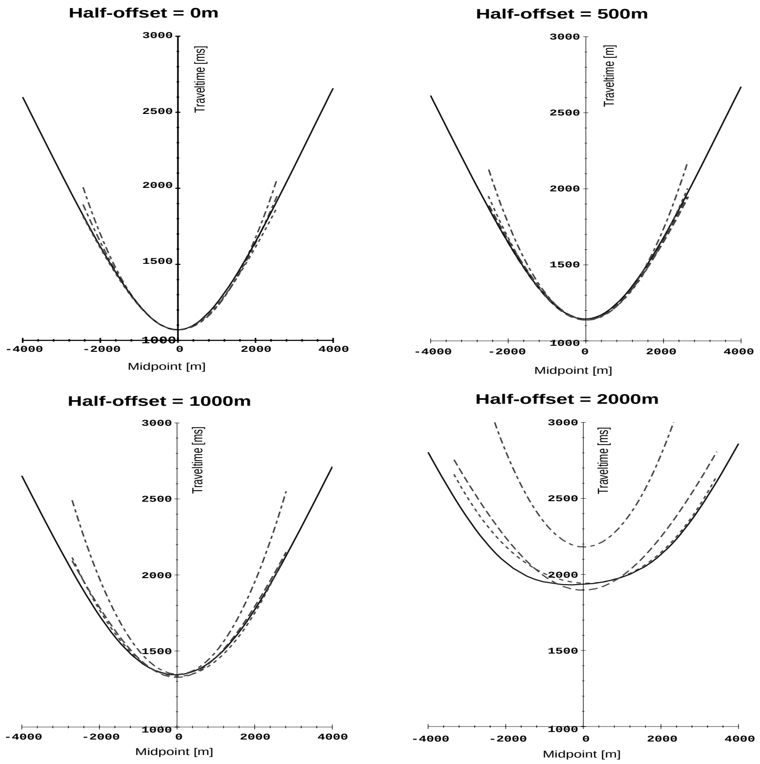

Figure 4: Shown are 2D cross-cuts for constant half-offsets of the four traveltime surfaces of Fig. 3. Displayed are the exact traveltime (solid line), the multi-focus traveltime (dotted line), the hyperbolic traveltime (dashed line) and the parabolic traveltime (dash-dotted line).

REFERENCES

Bortfeld, R., 1989, Geometrical ray theory: Rays and traveltimes in seismic systems (second-order approximation of the traveltimes): Geophysics, **54**, 342–349.

Gelchinsky, B., Berkovitch, A., and Keydar, S., 1997, Multifocusing homeomorphic imaging: Part 1. basic concepts and formulas: Karlsruhe workshop on amplitude-preserving seismic reflection imaging, Geophysical Institute Karlsruhe, Special Course on Homeomorphic Imaging, February, 1997 in Seeheim, Germany.

Hubral, P., 1983, Computing true-amplitude reflections in a laterally inhomogeneous earth: Geophysics, **48**, 1051–1062.

Schleicher, J., Tygel, M., and Hubral, P., 1993, Parabolic and hyperbolic paraxial two-point traveltimes in 3d media: Geophysical Prospecting, **41**, 495–513.

Tygel, M., Müller, T., Hubral, P., and Schleicher, J., 1997, Eigenwave based multiparameter traveltime expansions: 67th Ann. Internat. Mtg., Soc. Expl. Geophys., Expanded Abstracts, 1770–1773.

PUBLICATIONS

Detailed derivations of all presented traveltime expansion were published in (Tygel et al., 1997).